

PEDESTRIAN: An Egocentric Vision Dataset for Obstacle Detection on Pavements

Marios Thoma ^{1,2*}[†], Zenonas Theodosiou ^{1,3†},
 Harris Partaourides ⁴, Vassilis Vassiliades ¹, Loizos Michael ^{2,1},
 Andreas Lanitis ^{1,5}

¹*CYENS Centre of Excellence, Dimarchou Lellou Demetriadi 23,
 Nicosia, 1016, Cyprus.

²Open University Cyprus, Giannou Kranidioti 33, Nicosia, 2220, Cyprus.

³Department of Communication and Internet Studies, Cyprus University
 of Technology, Archiepiskopou Kyprianou 30, Limassol, 3036, Cyprus.

⁴AI Cyprus Ethical Novelties Ltd, Andrea Zakou 4, Limassol, 3095,
 Cyprus.

⁵Department of Multimedia and Graphic Arts, Cyprus University of
 Technology, Archiepiskopou Kyprianou 30, Limassol, 3036, Cyprus.

*Corresponding author(s). E-mail(s): m.thoma@cyens.org.cy;

Contributing authors: zenonas.theodosiou@cut.ac.cy;
harris.partaourides@ethicalaicy.com; v.vassiliades@cyens.org.cy;

loizos@ouc.ac.cy; andreas.lanitis@cut.ac.cy;

[†]These authors contributed equally to this work.

Abstract

Walking has always been a primary mode of transportation and is recognized as an essential activity for maintaining good health. Despite the need for safe walking conditions in urban environments, sidewalks are frequently obstructed by various obstacles that hinder free pedestrian movement. Any object obstructing a pedestrian's path can pose a safety hazard. The advancement of pervasive computing and egocentric vision techniques offers the potential to design systems that can automatically detect such obstacles in real time, thereby enhancing pedestrian safety. The development of effective and efficient identification algorithms relies on the availability of comprehensive and well-balanced datasets of egocentric data. In this work, we introduce the PEDESTRIAN dataset, comprising egocentric data for 29 different obstacles commonly found on urban sidewalks. A total of

340 videos were collected using mobile phone cameras, capturing a pedestrian's point of view. Additionally, we present the results of a series of experiments that involved training several state-of-the-art deep learning algorithms using the proposed dataset, which can be used as a benchmark for obstacle detection and recognition tasks. The dataset can be used for training pavement obstacle detectors to enhance the safety of pedestrians in urban areas.

Keywords: Pedestrian Safety, Egocentric Vision, Benchmark Tests

1 Introduction

Walking is a popular form of physical exercise, known for its positive impact on health. Being an aerobic and bone-strengthening activity, it can reduce the risk of chronic diseases and promote an active lifestyle [1]. Despite the widespread promotion of the benefits of walking by governments and health organizations, pedestrian safety continues to be a major concern, as road accidents pose a significant safety risk. The well-being of road users is influenced by numerous factors, such as speeding and rule violations by drivers, pedestrian negligence, and poor road conditions. Such conditions can be particularly hazardous for vulnerable groups like the elderly and disabled [2].

Poor road conditions, including inadequate lighting, poorly-maintained road surfaces, and obstructed pedestrian sidewalks are recognized to be some of the major factors contributing to road accidents [3]. Several studies have analyzed the behavior of pedestrians when faced with obstacles in their path. For example, in a study conducted by Ding et al. [4], the impact of different obstacle placements on pedestrian evacuation was examined. The results showed that the presence of obstacles in pedestrian pathways resulted in a significant delay before pedestrians could maneuver past the obstacles. Recent advancements in computer vision and mobile computing have paved the way for various applications aimed at enhancing the safety and well-being of pedestrians. Egocentric vision is a novel approach that utilizes data collected through wearable cameras or smartphones to enable real-time recognition of obstacles hindering safe walking within urban areas.

The work presented in this paper is a continuation of our previous work in this area [5], where automatic recognition of obstacles present in pedestrian pathways was addressed, focusing on the analysis of the performance of deep learning models under different conditions. However, to develop effective systems and applications for smartphones, large egocentric datasets are needed for developing the machine learning models [6]. Compared to our previous work in the area, the egocentric dataset was extended and, in this work, we present the PEDESTRIAN dataset, consisting of 340 videos collected on urban sidewalks and focusing on several types of obstacles impeding the safe movement of pedestrians. In total the PEDESTRIAN dataset includes 29 obstacle types, whereas in our previous work the dataset included 9 types. The data was collected by a smartphone user while walking around the city of Nicosia, Cyprus. Using the mobile camera, videos of the obstacles were collected from a pedestrian's

point of view. In addition to introducing the dataset, the performance of several state-of-the-art deep learning neural networks in obstacle detection using the dataset is also evaluated, setting benchmark standards for detection performance. The PEDESTRIAN dataset and related resources have been made publicly available to encourage further research in the area of obstacle detection on pavements, and the development of related applications.

The remainder of the paper proceeds with Section 2 providing an overview of the state-of-the-art research in the field of obstacle recognition and available egocentric datasets. Section 3 details the entire process of the dataset creation. In Section 4, the experimental procedure for evaluating the performances of benchmark tests, and the insights obtained from the evaluation are discussed. Finally, Section 5 summarizes our work, highlights its contributions, and suggests avenues for future enhancements.

2 Related Work

Egocentric vision is a perceptual method that involves the use of wearable cameras attached to a person to capture egocentric images or videos [7]. The advent of automatic egocentric data analysis has led to a plethora of applications designed to enhance daily human activities, not the least among them the augmentation of pedestrian safety. The use of Deep Learning (DL) is now the dominant approach for analyzing egocentric data. Thus, a wide range of egocentric datasets has been created and made publicly available for the training of DL models.

2.1 Pedestrian Safety

Various technologies have been developed with the aim to improve pedestrian safety. One such technology is ObstacleWatch, an obstacle detection model designed by Wang et al. [8], which uses acoustic signals emitted by smartphone speakers to determine the distance between the user and an obstacle. However, this approach proved to be inefficient due to the noise present in public spaces. Another application called LookUp was proposed by Jain et al. [9], which uses shoe-mounted inertial sensors to detect transitions from pedestrian walkways onto the road to alert texting pedestrians, achieved a detection rate of 90%. Liu et al. [10] developed a solution named InfraSee, which utilizes infrared sensors mounted on smartphones to detect hazardous situations and alerts the user. These approaches, however, necessitate additional equipment such as shoe-mounted sensors or infrared sensors, rendering them less practical for widespread adoption among the general public due to the extra hardware requirements and the inconvenience of carrying or wearing additional devices.

In contrast, smartphone-based applications offer a more practical and accessible solution for enhancing pedestrian safety without the need for supplementary equipment. WalkSafe, developed by Wang et al. [11], is a smartphone-based application that uses the smartphone's back camera to detect oncoming vehicles and alerts the user during active phone calls. The application uses decision trees to classify images and achieved an efficiency rate of 77%. A similar application, called Inspector, developed by Tang et al. [12], alerts users when they are approaching the edge of pedestrian areas. The model uses simple keypoint detection and K-means clustering for feature extraction

and uses Normal Bayes and K-nearest neighbors models to classify images with an accuracy rate of 92%–99%. TerraFirma, an application proposed by Jain and Gruteser [13], takes a different approach, choosing to identify the material composition of pedestrian walkways, instead of obstacles on the walkways themselves, in order to warn pedestrians when they transition from walkways to the street. Support Vector Machine classifiers were used to identify various ground surface types with an accuracy rate of 90%. Another application, AutoADAS, proposed by Wei et al. [14], uses smartphone cameras to detect objects in the environment and measure their distance from the user, warning them in case a potential collision is predicted. The application utilizes the user’s behavior profile collected from sensors on mobile devices, making it more personalized to the user. Similarly, Foerster et al. [15] developed SpareEye, an Android app that detects changes in the background of a mobile camera’s video stream and notifies the user when the distance between objects is reduced in each frame.

Hasan and Hasan [16] presented a comprehensive review of existing pedestrian safety models, highlighting the limitations and potential areas for further improvement. One of the issues highlighted was that, although various egocentric datasets are available, relatively few datasets focusing on pedestrian obstacle detection exist. One of the few such datasets available is that created by Theodosiou et al. [17], comprised of images of obstacles captured from a pedestrian’s perspective. The dataset was utilized to fine-tune a VGG16 model [18], achieving a training accuracy of 65% and validation accuracy of 55%. Subsequently, the fine-tuned VGG16 model was embedded in a smartphone application that aided pedestrians in capturing images of barriers they encountered and report their geographic location to the authorities, in order to enhance pedestrian safety [19]. Additionally, in Theodosiou et al. [20], three combinations of object detection models were trained using the aforementioned pedestrian-based image dataset, namely a Faster Region-Based CNN [21] using Inception-v2 [22] and ResNet-50 [23] for feature extraction, and a Single Shot MultiBox Detector (SSD) [24] using MobileNetV2 [25] for feature extraction. The models achieved, respectively, an average accuracy of 88.4%, 81.7% and 75.6%, demonstrating the dataset’s efficacy in training models to detect pedestrian obstacles on sidewalks.

2.2 Egocentric Visual Datasets

Several egocentric vision datasets have been developed for a variety of tests and applications, as depicted in Table 1. EPIC-Kitchens [26] is a benchmark egocentric video dataset focusing on kitchen activities. It consists of 100 hours of video data captured by head mounted cameras, while participants were performing various cooking tasks in kitchen environments. The dataset has been used for different purposes, such as action recognition, action detection and action anticipation. Ego4D [27] is a large-scale egocentric video dataset containing over 3670 hours of daily-life video captured from a wearable camera in diverse indoor and outdoor environments. The authors, in addition to the dataset, also proposed a series of benchmark tests for recall of past, present, and future activities. Charades-Ego [28] contains over 7500 files combining both first-person (actor) and third-person (observer) videos of daily activities, aiming to enable learning the connections between the two perspectives. EGTEA Gaze+ [29] consists of 28 hours of video data collected using a head-worn camera focusing on both

Table 1: Overview of available egocentric datasets.

Dataset	Camera		Year	Size	Task	Pedestrian Safety
	Wearable	Smartphone				
UT Egocentric [30]	✓	✗	2012	37 video hrs	Video Summarization	✗
Charades-Ego [28]	✓	✗	2018	7860 videos	Object & Action Recognition	✗
EgoGesture [32]	✓	✗	2018	2000 videos	Hand Gesture Recognition	✗
EGTEA Gaze+ [29]	✓	✗	2018	28 video hrs	Action & Gaze Recognition	✗
DR(eye)Ve [33]	✓	✗	2019	6.17 video hrs	Drivers' Focus Attention	✓
TerraFirma [13]	✓	✓	2019	9.25 video hrs	Surface Texture Recognition	✓
EGO-CH [34]	✓	✗	2020	27 video hrs	Visitors' Behavioral Understanding	✗
Theodosiou et al. [17]	✗	✓	2020	1796 frames	Obstacle Detection	✓
TREK-150 [35]	✓	✗	2021	150 videos	Object Tracking	✗
Ego4D [27]	✓	✗	2022	3670 video hrs	Memory Recall	✗
EPIC-Kitchens [26]	✓	✗	2022	100 video hrs	Object & Action Recognition	✗
EgoObjects [31]	✓	✗	2023	>9000 videos	Object Understanding	✗
PEDESTRIAN	✗	✓	2024	82120 frames	Obstacle Detection	✓

activities and gazes of the subjects. The UT egocentric dataset [30] consists of 37 video hours collected through wearable cameras. The collection concerns the daily lives of 4 different wearers and the dataset was initially used for video summarization based on the people and objects discovered in each event.

Different object categories are included in the EgoObjects dataset [31] which was created for object understanding in egocentric visual data. The dataset covers 250 object categories in more than 9000 video files. A large amount of video gestures were collected in the EgoGesture dataset [32]. The gestures were gathered from a first-person point of view using 50 human subjects. The TerraFirma dataset [13] is concerned with images of sidewalks' surfaces from a pedestrian point of view. The data was collected using smartphone cameras from volunteers walking in various cities. In addition, other purpose datasets have been proposed, such as the DR(eye)Ve [33] for driving, EGO-CH [34] for cultural sites, TREK-150 [35] for object tracking, etc.

Apart from the dataset presented in Theodosiou et al. [17], which had several limitations concerning its size, to our knowledge no other dataset has been proposed for the protection of pedestrians from the various obstacles that crowd sidewalks. Although there are egocentric datasets that can be used to protect pedestrians, including datasets of objects, people driving and sidewalk surface textures, none focuses exclusively on the obstacles that obstruct the free movement and endanger the lives of pedestrians.

2.3 Obstacle Detection in Egocentric Datasets

Various DL architectures, including Convolutional Neural Networks (CNNs), have been deployed with notable effectiveness in egocentric and mobile computing applications. The constraints imposed by smartphone hardware necessitated the creation of the MobileNetV2 framework [25], which is tailored specifically for these environments through the prioritization of compact model dimensions and reduced inference latency. MobileNetV2, distinguished by its innovative inverted residual structure as detailed by Sandler et al. [25], represents a prominent advancement in CNN designs optimized for mobile platforms, offering enhanced efficiency in tasks such as image classification. This architecture innovatively employs an expansion of low-dimensional features,

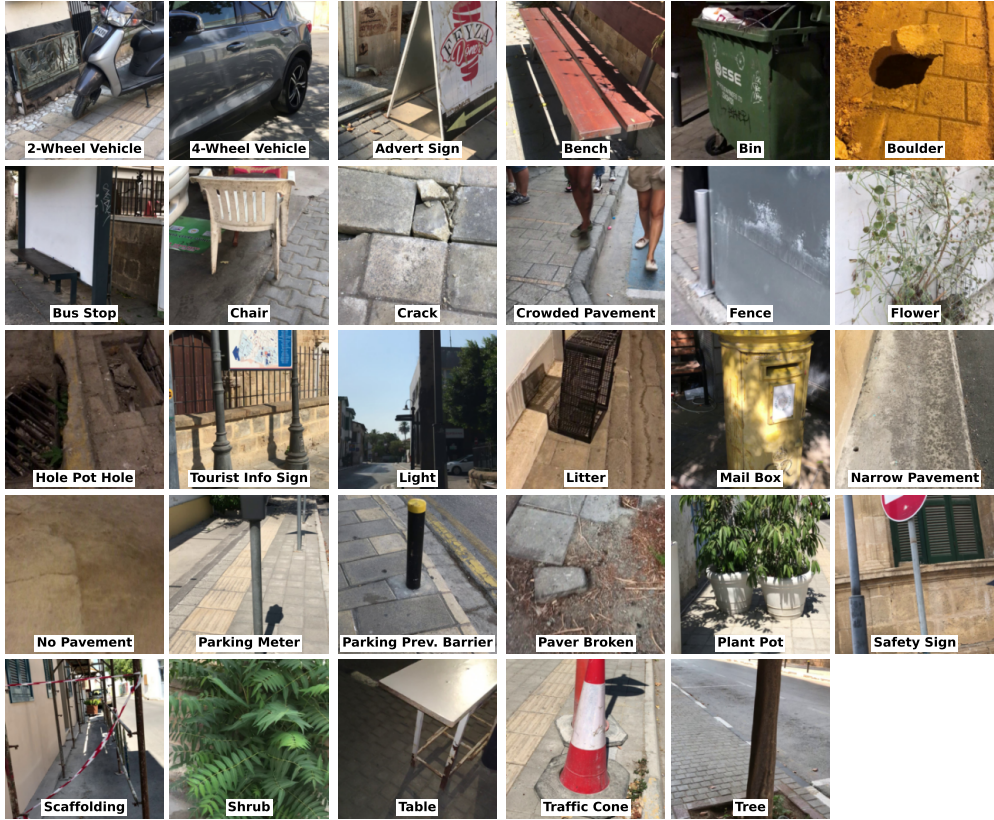


Fig. 1: Example images for the 29 obstacle types in the PEDESTRIAN dataset.

followed by a reduction in dimensionality via depth-wise convolution, optimizing both computational resource usage and performance.

Despite the success of CNN-based models such as **MobileNetV2** (and its successors, **MobileNetV3-Small** and **MobileNetV3-Large** [36]), the pursuit for models that offer superior accuracy performance has led to the development of **Vision Transformer** (ViT) based architectures, as introduced by Dosovitskiy et al. [37]. These architectures diverge from traditional CNN approaches by leveraging self-attention mechanisms [38], a methodology that, rather than focusing on computational efficiency, aims to enhance the model’s accuracy in various computer vision tasks, including image classification and object recognition. The ViT architecture represents a significant shift in the field, positioning itself as a competitive alternative to the previously dominant CNN models, by potentially offering improvements in accuracy for certain applications.

3 The PEDESTRIAN Dataset

In this work, we aim to create and make publicly available a new comprehensive visual dataset related to pedestrian safety, to address a gap in the related literature. In this

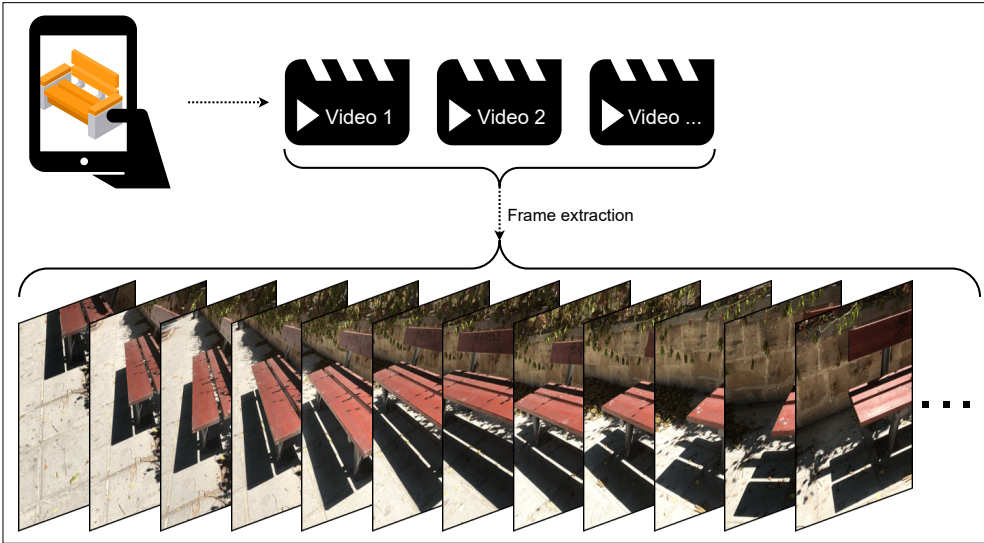


Fig. 2: Pipeline for the generation of the PEDESTRIAN dataset: multiple videos of each obstacle type were taken using a smartphone camera from a pedestrian’s point of view, and then individual frames were extracted from the collected videos.

section, we describe the methodology we followed to create the new PEDESTRIAN dataset, and give an overview of the created dataset. Detailed instructions on how to obtain the dataset are included in Appendix A.1.

3.1 Data Collection

The PEDESTRIAN dataset is composed of video files showcasing obstacles that endanger the safety of pedestrians when walking in the city of Nicosia, Cyprus. Proper identification of obstacles requires special attention to various considerations: defining the different obstacle types, assessing the degree of danger they pose, and determining in what context a simple object can be considered an obstacle. Thus, the problems related to pedestrian safety in modern cities were studied, and the various kinds of obstacles observed on city sidewalks were identified before collecting the data. In total, 29 different types of obstacles (see Figure 1) were identified and used for data collection.

Obstacles were grouped into 3 high-level categories: (i) *Physical Condition*, (ii) *Infrastructure*, and (iii) *Temporary*, as illustrated in Figure 3. The *Physical Condition* category includes obstacles related to poor pavement maintenance, which is further divided into 2 subcategories. The *Infrastructure* category includes obstacles related to parts of the infrastructure that affect safe traffic on a sidewalk or part of the sidewalk and consists of 3 subcategories. Finally, the *Temporary* category concerns all temporary obstacles that affect the safety of sidewalks and concerns 3 subcategories.

The data collection process was carefully designed to guarantee a dataset that is both comprehensive and varied, particularly in terms of natural lighting conditions. We compiled the dataset by recording videos, each focusing on a distinct obstacle type.

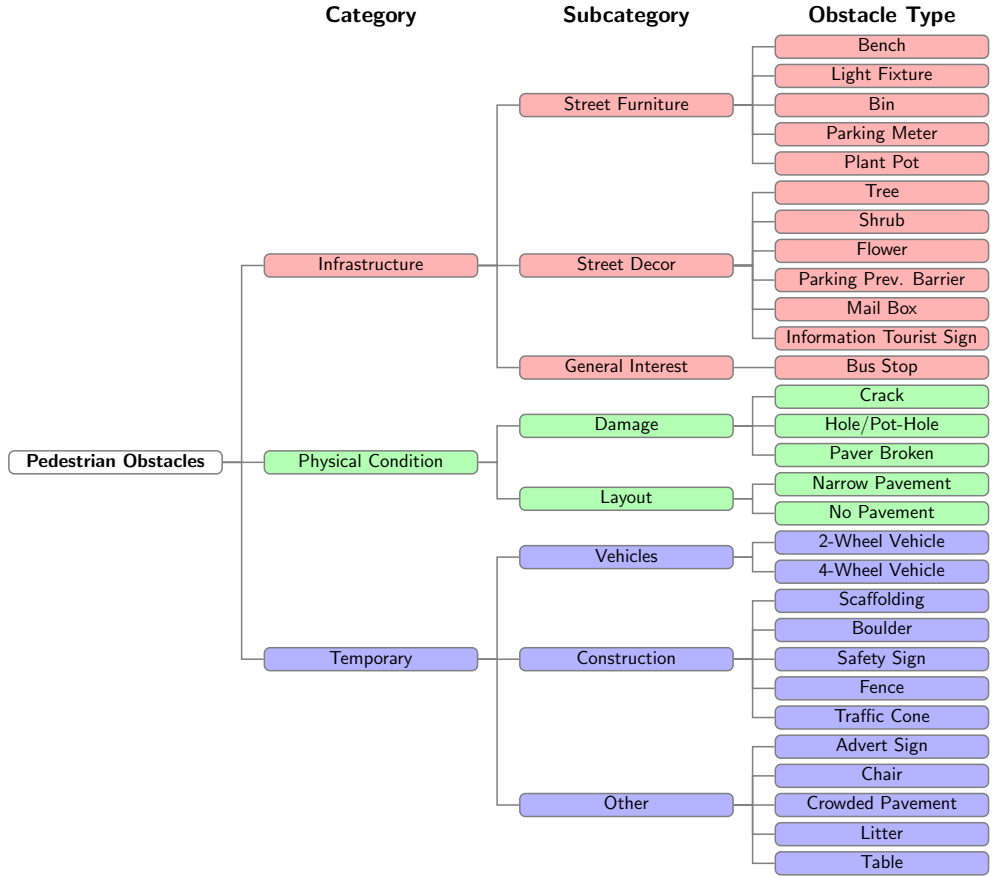


Fig. 3: The taxonomy of obstacle types included in the dataset.

Subsequently, we extracted individual frames from these videos to create the dataset, as illustrated in Figure 2. This approach ensured that each video precisely showcased a single obstacle, enabling us to efficiently capture the wide range of barriers encountered in urban environments with a high degree of control and accuracy.

The data collection process was facilitated by the use of a simple and low-cost setup, comprising of smartphone cameras. Two smartphone models were used, in order to prevent DL models overfitting on the characteristics of a single capture device. Specifically, the cameras of the smartphones Xiaomi Mi Mix 3 and Apple iPhone 7 were used. The videos from both smartphone cameras were captured at chest height, simulating the point of view of a wearable camera worn by a pedestrian. The dataset consists of 340 videos, covering the 29 predefined obstacle types, under 3 different lighting conditions: daytime with sunlight, cloudy day, and night. Data collection was followed by a processing step to resolve privacy issues and comply with the EU General Data Protection Regulation (GDPR) [39], which included face, car license plate, and signs blurring.

Table 2: Number of videos, total video length and available frames per *Category* and lighting condition.

Category	Video Count				Total Video Length (s)				Frame Count			
	Day	Night	Cloudy	Total	Day	Night	Cloudy	Total	Day	Night	Cloudy	Total
Infrastructure	53	53	47	153	361	346	321	1029	10832	14863	10115	35810
Physical Condition	20	19	20	59	128	138	150	417	3867	6777	4507	15151
Temporary	44	44	40	128	339	299	246	885	10185	11984	8990	31159
Total	117	116	107	340	829	784	718	2332	24884	33624	23612	82120

Table 3: Number of videos, total video length (in seconds) and available frames per *Subcategory* and lighting condition.

Subcategory	Video Count				Total Video Length (s)				Frame Count			
	Day	Night	Cloudy	Total	Day	Night	Cloudy	Total	Day	Night	Cloudy	Total
Construction	16	16	17	49	149	109	103	361	4485	3716	3541	11742
Damage	13	11	11	35	78	79	62	220	2367	4082	1878	8327
General Interest	2	2	2	6	13	26	26	66	400	1602	805	2807
Layout	7	8	9	24	50	59	87	197	1500	2695	2629	6824
Other	18	19	16	53	116	118	80	315	3498	4752	2886	11136
Street Decor	27	29	26	82	183	189	168	542	5509	7407	5219	18135
Street Furniture	24	22	19	65	164	130	125	420	4923	5854	4091	14868
Vehicles	10	9	7	26	73	72	63	208	2202	3516	2563	8281
Total	117	116	107	340	829	784	718	2332	24884	33624	23612	82120

3.2 Dataset Description

A breakdown of the dataset statistics for the 3 taxonomy levels, and a breakdown across lighting conditions are shown in Tables 2, 3, and 4, respectively.

The total number of videos per *Obstacle type* are presented in Figure 4a. Figure 4b shows a histogram of video duration, which varies from 1s to 17s. Overall, the dataset consists of a total of 82120 images. Figure 5a–c shows a visual breakdown of the number of images per taxonomy level.

All videos in the dataset have a Full HD resolution of 1080×1920 pixels (portrait orientation). The default settings for video frame rates (frames-per-second, FPS) for the two smartphones were used: 60 FPS for the Mi Mix 3 and 30 FPS for the iPhone 7. Table 5 shows of a breakdown of the dataset statistics based on smartphone model (and by proxy, FPS).

4 Benchmark Experiments

A diverse set of benchmarking experiments was performed to evaluate the utility of the new PEDESTRIAN dataset presented in this work. Specifically, a number of pretrained DL model architectures were fine-tuned on a balanced subset of the dataset, to evaluate its performance. See Appendix A.2 for details.

Table 4: Number of videos, total video length (in seconds) and available frames per *Obstacle type* and lighting condition.

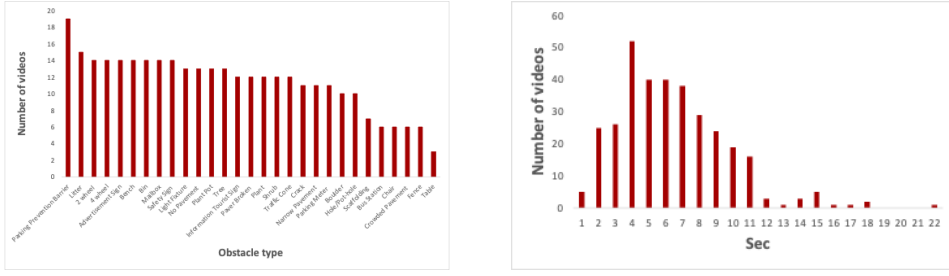
Obstacle type	Video Count				Total Video Length (s)				Frame Count				
	Day	Night	Cloudy	Total	Day	Night	Cloudy	Total	Day	Night	Cloudy	Total	
2-Wheel Vehicle	6	5	3	14	34	25	20	79	1022	1533	607	3162	
4-Wheel Vehicle	4	4	4	12	39	46	42	128	1180	1983	1956	5119	
Advert Sign	6	4	4	14	45	27	13	86	1362	1146	410	2918	
Bench	6	4	4	14	43	24	35	103	1309	1487	1059	3855	
Bin	6	5	3	14	37	23	14	75	1138	1070	428	2636	
Boulder	2	4	4	10	9	28	18	56	296	845	551	1692	
Bus Stop	2	2	2	6	13	26	26	66	400	1602	805	2807	
Chair	2	2	2	6	13	10	7	31	410	622	226	1258	
Crack	4	4	3	11	23	31	26	82	715	1902	800	3417	
Crowded Pavement	2	2	2	6	8	4	7	20	259	213	222	694	
Fence	2	2	2	6	20	18	18	57	617	551	549	1717	
Flower	2	6	4	12	16	35	34	85	485	1410	1025	2920	
Hole/Pot-Hole	4	4	4	12	22	23	16	63	686	1045	497	2228	
Information Tourist Sign	4	4	4	12	28	26	20	75	851	802	613	2266	
Light Fixture	4	4	5	13	23	24	36	84	700	1059	1396	3155	
Litter	4	7	4	15	29	54	24	107	874	1867	1194	3935	
Mail Box	4	6	4	14	20	46	23	90	613	1791	697	3101	
Narrow Pavement	3	4	4	11	23	30	38	92	708	1343	1143	3194	
No Pavement	4	4	5	13	26	28	49	104	792	1352	1486	3630	
Parking Meter	4	4	3	11	30	23	21	75	926	963	646	2535	
Parking Prev. Barrier	6	6	7	19	35	33	40	109	1069	1305	1365	3739	
Paver Broken	5	3	4	12	32	23	19	75	966	1135	581	2682	
Plant Pot	4	5	4	13	13	28	33	18	81	850	1275	562	2687
Safety Sign	4	4	6	14	28	20	36	86	870	871	1533	3274	
Scaffolding	4	2	1	7	55	22	7	85	1670	670	239	2579	
Shrub	6	3	3	12	53	23	20	97	1590	1106	618	3314	
Table	4	4	4	12	19	20	27	68	593	904	834	2331	
Traffic Cone	4	4	4	12	34	19	22	75	1032	779	669	2480	
Tree	5	4	4	13	30	23	30	83	901	993	901	2795	
Total	117	116	107	340	829	784	718	2332	24884	33624	23612	82120	

Table 5: Number of videos, total video length (in seconds) and available frames per smartphone model (and by extension, frame rate) and lighting condition.

Camera model	Video Count				Total Video Length (s)				Frame Count			
	Day	Night	Cloudy	Total	Day	Night	Cloudy	Total	Day	Night	Cloudy	Total
iPhone 7 (30 FPS)	117	60	98	275	829	448	650	1927	24884	13445	19508	57837
Mi Mix 3 (60 FPS)	0	56	9	65	0	336	68	405	0	20179	4104	24283
Total	117	116	107	340	829	784	718	2332	24884	33624	23612	82120

4.1 Balanced Dataset Subset

To facilitate the benchmark experiments, and to ensure a balanced dataset in terms of images per *Obstacle type*, we extracted a subset from the PEDESTRIAN dataset described in the previous sections, using the pipeline shown in Figure 2. For each obstacle type, a fixed number of images c was extracted from the total number of available frames per obstacle type, n , ensuring that $c \leq n$ for all types. Given that each obstacle type had a different number of frames available (refer to Table 4), the



(a) Number of videos per obstacle type

(b) Histogram of video duration

Fig. 4: Statistics of the dataset.

Table 6: Model architectures used in the fine-tuning experiments. For all models ImageNet-1K pretrained weights provided by PyTorch were used (links to the weights and model recipes are provided). Accuracies are reported on the ImageNet-1K dataset using single crops. The models are sorted in ascending order in regards to their number of parameters (in millions).

Model Name	Top-1 Acc. (%)	Top-5 Acc. (%)	Params (M) \uparrow	Weights	Model Recipe	Citation
MobileNetV3-Small	67.67	87.40	2.5	link	link	[36]
MobileNetV2	71.88	90.29	3.5	link	link	[25]
EfficientNet-B0	77.69	93.53	5.3	link	link	[40]
MobileNetV3-Large	74.04	91.34	5.5	link	link	[36]
GoogLeNet	69.78	89.53	6.6	link	link	[41]
DenseNet-121	74.43	91.97	8.0	link	link	[42]
ResNet-18	69.76	89.08	11.7	link	link	[23]
DenseNet-201	76.90	93.37	20.0	link	link	[42]
EfficientNetV2-S	84.23	96.88	21.5	link	link	[43]
ResNet-34	73.31	91.42	21.8	link	link	[23]
ResNet-50	76.13	92.86	25.6	link	link	[23]
ResNet-101	77.37	93.55	44.5	link	link	[23]
ConvNeXt-Small	83.62	96.65	50.2	link	link	[44]
ResNet-152	78.31	94.05	60.2	link	link	[23]
ConvNeXt-Base	84.06	96.87	88.6	link	link	[44]
ConvNeXt-Large	84.41	96.98	197.8	link	link	[44]

frames were selected as follows:

$$\text{frame selection}(n, c) = \begin{cases} \text{uniformly at random,} & \text{if } 1 \leq \frac{n}{c} < 2, \\ \text{regularly at intervals of } \lfloor \frac{n}{c} \rfloor, & \text{if } \frac{n}{c} \geq 2. \end{cases}$$

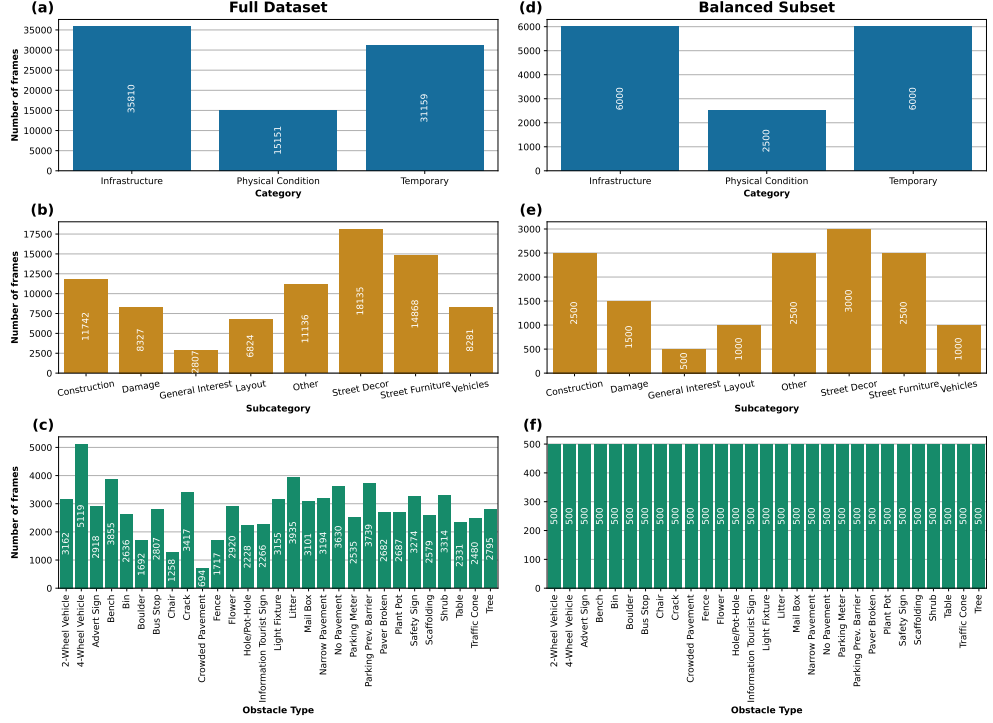


Fig. 5: Breakdown of the number of frames in the full PEDESTRIAN dataset for the three taxonomy levels: (a) *Category*, (b) *Subcategory*, and (c) *Obstacle type*; and, respectively, (d–f) for the balanced subset used in the benchmarking experiments.

For the regular interval selection, the selection process started from the first frame available (index 0 of the concatenated frames from all videos for each obstacle type), and continued at intervals of $\lfloor \frac{n}{c} \rfloor$.

To create the balanced subset, $c = 500$ was chosen, that accommodates the minimum available number of frames for the obstacle type *Crowded Pavement* ($n = 694$, see Table 4). Thus, the size of the balanced subset of PEDESTRIAN that was used for the fine-tuning experiments was $29 \times 500 = 14500$ images. Figure 5d–f shows a visual breakdown of the number of images per taxonomy level in the balanced subset (note that while the balancing was done only in terms of images per *Obstacle type*, and not for the other two taxonomy levels).

4.2 Model Fine-tuning

A total of 16 DL architectures, listed in Table 6, were fine-tuned using the balanced subset described in the previous section. Effort was made to include state-of-the art model architectures, especially in regards to parameter size: the smallest model used in terms of parameters was MobileNetV3-Small at 2.5M parameters [36], while the largest was ConvNeXt-Large at 197.8M parameters [44]. The pretrained weights of the

models using the ImageNet dataset [45, 46], that are available through the PyTorch library (links provided in Table 6), were used.

Each of the architectures was fine-tuned to identify the obstacles at all three taxonomy levels (*Category*, *Subcategory* and *Obstacle type*). In addition, the models were trained by either freezing all their layers apart from the last, or without freezing any of their layers. A random split of the dataset into 70% training, 20% validation and 10% testing subsets was performed before training. Training was performed for 30 epochs, with batches of 32 images, using the Adam optimizer [47] and a learning rate of 0.001. The default pre-processing transforms provided by the model recipes (see Table 6) were applied to the input images during training and testing.

For each training combination of DL architecture and taxonomy level, the experiments were repeated 5 times, using a different random seed for the splitting into training/validation/testing subsets. The same sequence of random seeds was used for each combination, to enable one-to-one comparisons between combinations. Thus, a total of 16 DL architectures \times 3 tax. levels \times 2 layer freezing status \times 5 reps = 480 fine-tuning experiments were performed.

4.3 Experimental Results

The results obtained from the fine-tuning of the 16 DL models utilizing the PEDESTRIAN dataset at all three taxonomy levels are summarized in Figure 6 and Table 7. (Detailed results, broken down per *Obstacle type*, are provided in Appendix B, Tables B1 & B2). These results include the outcomes from experiments both with and without freezing the layers of the models. The primary objective of these experiments was to assess the effectiveness of the new PEDESTRIAN dataset across a diverse range of DL architectures.

At the *Obstacle type* level, all models produced very good results, with accuracies over 99%. ConvNeXt-Small [44] had a slight advantage with 99.96% accuracy with its layers frozen, while EfficientNetV2-S [43] led with 99.89% accuracy without layer freezing. On the lower end, ResNet-152 and ResNet-18 [23] achieved 99.52% and 99.33% respectively, the former with unfrozen layers and the latter with layers frozen.

For the *Obstacle type* level, the impact of freezing the layers on model accuracy was negligible. In contrast, for the *Category* and *Subcategory* levels, allowing the layers to remain unfrozen generally yielded better results. Specifically, at the *Category* level, EfficientNet-B0 [40] achieved the highest accuracy of 99.90% with unfrozen layers, while ConvNeXt-Large [44] topped the frozen layers category with 99.61% accuracy. For the *Subcategory* level, EfficientNetV2-S reached the highest unfrozen accuracy at 99.92%, and ConvNeXt-Large again performed best for the models with frozen layers at 99.86%.

The observed discrepancy in model performance between the *Category* and *Subcategory* levels, as compared to the *Obstacle type* level, may stem from several factors. It was noted that networks with fewer parameters were, in general, less adept at handling the complexity required for *Category* and *Subcategory* classification tasks. This struggle may be partially attributed to an imbalance within the dataset for these taxonomy levels, since even though the subset used was balanced in terms of number of frames for the taxonomy level *Obstacle type* (Figure 5f), it was not balanced for the other two

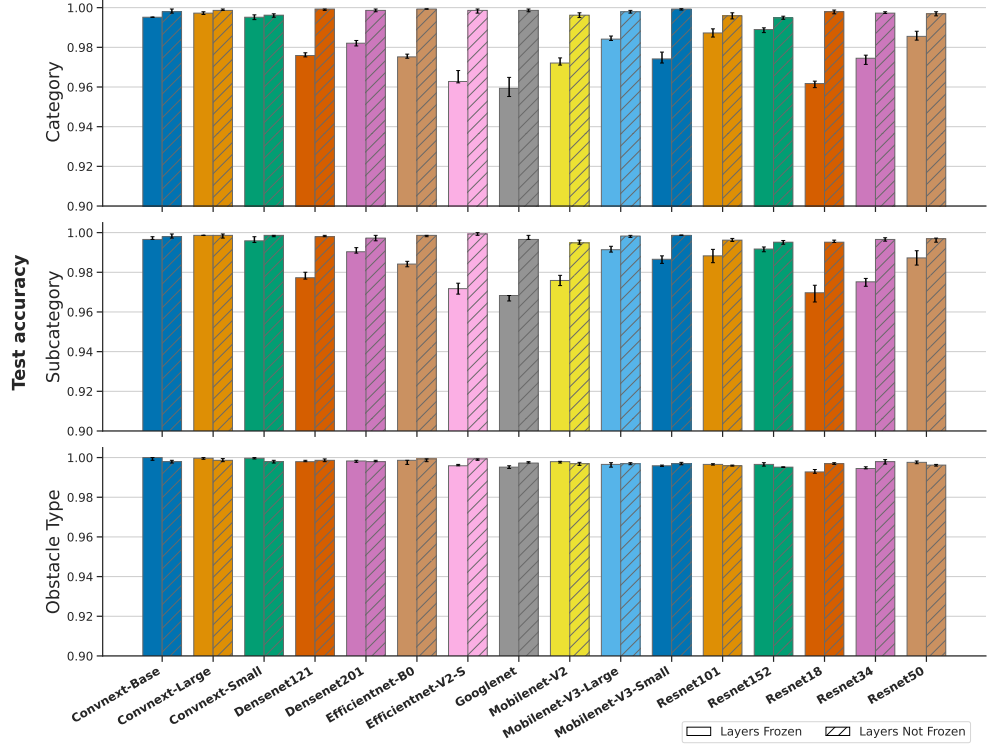


Fig. 6: Benchmark results for the fine-tuning of the 16 DL models using the PEDESTRIAN dataset, on all 3 taxonomy levels, *with* model layer freezing (bars with no hatches) or *without* layer freezing (bars with hatches). The fine-tuning took place over 30 epochs; the median test accuracy results for the best epoch of each training combination are shown, over 5 repetitions that were run for each combination. The error bars show the Q1–Q3 interval. The y-axis scale is truncated to range [0.9, 1.0] to make the differences between models more immediately obvious.

levels (Figure 5d & 5e). Furthermore, the difference in performance can potentially be explained by the necessity for the networks to abstract and learn more complex features to accurately classify data at the *Category* and *Subcategory* levels. These factors suggest that the *Category* and *Subcategory* levels present inherently more challenging classification problems, revealing a discernible discrepancy in model efficacy across taxonomy levels.

The results gathered from the series of experiments were, in general, excellent. The performance metrics indicated that the PEDESTRIAN dataset is robust and enables the DL models to achieve high levels of accuracy. Across different architectures, there was a consistent trend of models being able to effectively recognize and classify the data, regardless of the taxonomic level considered. This underlines the PEDESTRIAN dataset's quality and its utility in training DL models for pedestrian obstacle detection and classification tasks.

Table 7: Benchmark results for the fine-tuning of the 16 DL models using the PEDESTRIAN dataset, on all 3 taxonomy levels, either with frozen (F) or not frozen (NF) model layers. The mean test accuracy results for the best epoch of each training combination are shown, averaged over the 5 repetitions that were run for each combination. The min and max values for each column are highlighted in *italics* and **bold**, respectively.

Model Name	Category		Subcategory		Obstacle Type	
	NF	F	NF	F	NF	F
ConvNeXt-Small	99.586	99.509	99.793	99.612	99.747	99.959
ConvNeXt-Base	99.793	99.545	99.821	99.738	99.807	99.931
ConvNeXt-Large	99.848	99.614	99.807	99.862	99.879	99.948
DenseNet-121	99.862	97.626	99.809	97.810	99.847	99.801
DenseNet-201	99.848	98.208	99.711	99.076	99.779	99.793
EfficientNet-B0	99.904	97.491	99.821	98.346	99.876	99.793
EfficientNetV2-S	99.821	96.485	99.917	97.161	99.890	99.614
GoogLeNet	99.835	<i>95.879</i>	99.724	<i>96.637</i>	99.766	99.531
MobileNetV2	99.621	97.364	99.552	97.588	99.673	99.742
MobileNetV3-Large	99.793	98.501	99.793	99.190	99.690	99.604
MobileNetV3-Small	99.897	97.553	99.879	98.622	99.707	99.586
ResNet-18	99.776	96.089	99.604	96.881	99.707	<i>99.328</i>
ResNet-34	99.776	97.295	99.655	97.467	99.776	99.518
ResNet-50	99.690	98.622	99.552	98.725	99.604	99.759
ResNet-101	99.586	98.725	99.638	98.811	99.604	99.655
ResNet-152	<i>99.500</i>	98.828	<i>99.500</i>	99.139	<i>99.518</i>	99.655

5 Conclusions

This work addresses the critical issue of pedestrian safety, which remains a significant concern globally, due to the risks posed by road accidents. Recognizing the lack of specialized resources for enhancing pedestrian safety through obstacle detection and avoidance, we introduced the PEDESTRIAN dataset, a novel egocentric vision dataset specifically designed for identifying obstacles that pedestrians commonly encounter in modern urban environments. The dataset comprises of 340 videos, collected and processed to represent 29 distinct types of obstacles under various lighting conditions, using smartphone cameras to simulate a pedestrian’s point of view. This effort marks a significant step towards leveraging advanced machine learning techniques, particularly deep learning, to improve pedestrian safety by providing a comprehensive dataset that captures the complexity and diversity of urban pedestrian obstacles.

To demonstrate the utility and effectiveness of the PEDESTRIAN dataset, we conducted a series of benchmark experiments involving the fine-tuning of 16 different deep learning architectures on the dataset. These experiments were designed to evaluate the dataset’s performance across three taxonomic levels of obstacle classification: *Category*, *Subcategory* and *Obstacle type*. By performing fine-tuning with both frozen

and unfrozen model layers, we aimed to explore the adaptability and learning capabilities of various architectures when applied to the task of pedestrian obstacle detection. The benchmark experiments served a dual purpose: firstly, to validate the PEDESTRIAN dataset as a robust tool for training and enhancing obstacle detection models, and secondly, to provide insights into the effectiveness of different deep learning architectures for egocentric vision tasks in urban pedestrian settings. Through these experiments, we established a comprehensive evaluation framework that underscores the dataset’s potential to advance research and development in pedestrian safety technologies.

The PEDESTRIAN dataset has great potential for developing effective applications and systems to enhance the safety of citizens as they navigate city sidewalks, especially given the increased distractions from mobile phone use. Additionally, this dataset can aid in creating systems that assist individuals using mobility aids, including those with mobility impairments and the elderly, ensuring their comfortable and safe movement on urban sidewalks.

In future work, several directions could be pursued to enhance the capabilities and applications of pedestrian safety technologies. Expanding the PEDESTRIAN dataset to cover a wider array of environments and conditions would be beneficial for improving the robustness of obstacle detection models. The collection of images from other cities/countries is one of the main future goals for expanding this work. Synergies with partners in other countries will be explored to enrich the dataset. Incorporating additional data types, such as audio and sensor data, could also enrich the dataset and enable more comprehensive obstacle detection solutions. Moreover, investigating the use of federated learning could facilitate the collaborative enhancement of models while addressing privacy concerns. Collaboration with urban planners could also provide insights into practical implementations of these technologies. These future research directions underscore the importance of continued exploration and interdisciplinary collaboration to advance pedestrian safety technologies.

In conclusion, this work presents the PEDESTRIAN dataset, a new egocentric dataset focused on pedestrian safety. A suite of benchmark experiments using different deep learning models show the dataset’s usefulness for the development of effective obstacle detection systems. The main importance of this work is its contribution to the goal of making pedestrian environments safer, setting the stage for future advancements in this essential field.

Declarations

Funding. This project has received funding from the European Union’s Horizon 2020 Research and Innovation Programme, under Grant Agreement No 739578, complemented by the Government of the Republic of Cyprus through the Directorate General for European Programmes, Coordination and Development.

Conflict of Interest. On behalf of all authors, the corresponding author states that there is no conflict of interest.

Appendix A Dataset & Benchmarks

A.1 Dataset Availability

The PEDESTRIAN dataset has been made publicly available to facilitate reproducibility and encourage further research in pedestrian safety [48]. The complete dataset, including all video files and the balanced benchmark subset, is distributed as a 5.9 GB **zip** archive through Zenodo (DOI: [10.5281/zenodo.10907945](https://doi.org/10.5281/zenodo.10907945)). Detailed instructions for accessing and using the dataset are provided in the accompanying **README** file included in the archive.

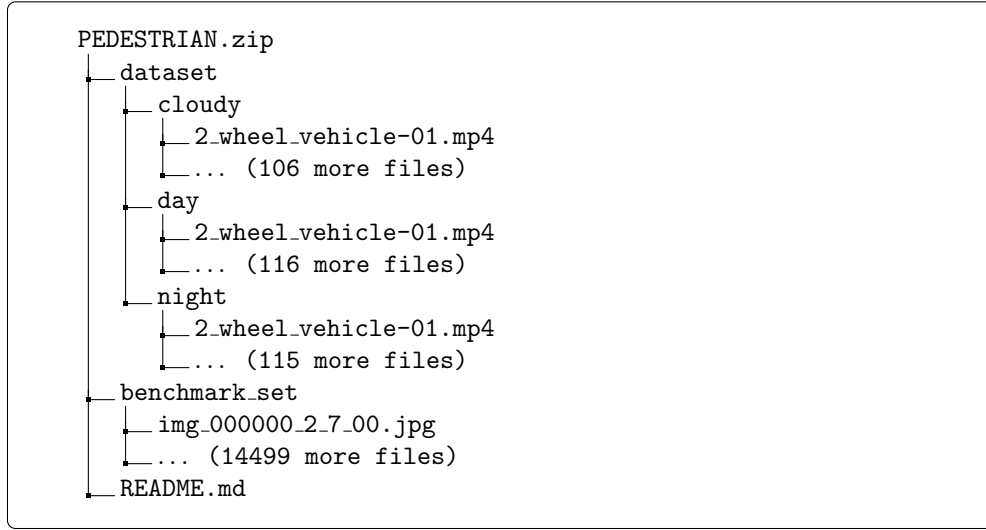


Fig. A1: The directory structure of the dataset.

The dataset's directory structure is shown in Figure A1. The `dataset/` subfolder contains the full PEDESTRIAN dataset organized by lighting condition (`cloudy/`, `day/`, `night/`), with each video file stored in its respective condition folder. The `benchmark_set/` subfolder contains a balanced subset of the dataset in terms of *Obstacle type* (see Section 4.1 for more information), as individual frames extracted from the videos.

A.2 Benchmark Experiments

All the relevant source code for working with the dataset is publicly available at [this GitHub repository](#), which includes:

- Source code that can be used to replicate the benchmark experiments presented in Section 4.
- Implementations of PyTorch `Dataset` classes, to allow for easy loading and integration of the dataset into existing PyTorch training pipelines.

Appendix B Detailed Results

Tables B1 & B2 show test accuracy results for all 16 DL models per *Obstacle type*.

Table B1: Test accuracy per obstacle type for the first 8 DL models (F: Frozen layers, NF: Not-frozen layers).

Obstacle Type	Convnext Base		Convnext Large		Convnext Small		Densenet121		Densenet201		Efficientnet B0		Efficientnet V2 S		Googlenet	
	F	NF	F	NF	F	NF	F	NF	F	NF	F	NF	F	NF	F	NF
2-Wheel Vehicle	1.000	1.000	1.000	1.000	1.000	1.000	1.000	1.000	1.000	1.000	1.000	1.000	1.000	1.000	1.000	1.000
4-Wheel Vehicle	1.000	1.000	1.000	1.000	1.000	1.000	0.998	1.000	1.000	1.000	1.000	0.988	1.000	1.000	1.000	1.000
Advert Sign	1.000	1.000	1.000	1.000	0.996	1.000	1.000	1.000	1.000	1.000	1.000	0.996	1.000	0.996	1.000	1.000
Bench	1.000	1.000	1.000	1.000	1.000	1.000	1.000	1.000	1.000	1.000	1.000	1.000	1.000	1.000	1.000	1.000
Bin	1.000	1.000	1.000	1.000	1.000	1.000	1.000	1.000	1.000	1.000	1.000	1.000	1.000	1.000	1.000	1.000
Boulder	1.000	1.000	1.000	1.000	1.000	1.000	1.000	1.000	1.000	1.000	1.000	0.996	1.000	1.000	1.000	1.000
Bus Stop	1.000	0.996	1.000	1.000	1.000	1.000	1.000	1.000	1.000	1.000	1.000	0.996	1.000	1.000	1.000	0.996
Chair	1.000	1.000	1.000	1.000	1.000	1.000	0.998	1.000	1.000	1.000	1.000	1.000	1.000	1.000	1.000	1.000
Crack	1.000	1.000	1.000	1.000	0.998	0.998	1.000	1.000	1.000	1.000	1.000	1.000	1.000	1.000	1.000	1.000
Crowded Pavement	1.000	1.000	1.000	1.000	1.000	1.000	1.000	1.000	1.000	1.000	1.000	1.000	1.000	1.000	1.000	1.000
Fence	1.000	1.000	1.000	1.000	1.000	1.000	1.000	1.000	1.000	1.000	1.000	1.000	1.000	1.000	1.000	1.000
Flower	1.000	0.996	1.000	1.000	1.000	1.000	1.000	1.000	1.000	1.000	1.000	0.996	1.000	0.976	1.000	1.000
Hole/Pot-Hole	1.000	0.996	1.000	0.995	1.000	0.996	1.000	1.000	1.000	1.000	1.000	0.996	1.000	0.996	1.000	0.996
Information Tourist Sign	1.000	1.000	1.000	1.000	1.000	1.000	1.000	1.000	1.000	1.000	1.000	1.000	1.000	1.000	1.000	1.000
Light Fixture	1.000	0.992	1.000	1.000	1.000	0.998	1.000	1.000	0.995	0.992	0.996	0.992	0.992	0.996	0.992	1.000
Litter	1.000	0.992	1.000	0.995	1.000	0.996	0.996	0.996	0.995	0.996	0.996	0.996	0.996	0.996	0.992	0.996
Mail Box	1.000	1.000	1.000	1.000	1.000	1.000	1.000	1.000	1.000	1.000	1.000	1.000	1.000	1.000	1.000	1.000
Narrow Pavement	1.000	1.000	1.000	1.000	1.000	1.000	1.000	1.000	1.000	1.000	1.000	1.000	1.000	1.000	1.000	1.000
No Pavement	1.000	1.000	1.000	1.000	1.000	0.998	0.996	1.000	0.995	1.000	0.992	1.000	1.000	0.996	0.984	1.000
Parking Meter	1.000	1.000	1.000	1.000	1.000	1.000	1.000	1.000	1.000	1.000	1.000	1.000	1.000	1.000	0.996	1.000
Parking Prev. Barrier	1.000	1.000	1.000	1.000	1.000	1.000	1.000	1.000	1.000	1.000	1.000	1.000	1.000	1.000	0.996	1.000
Paver Broken	1.000	1.000	1.000	1.000	1.000	0.998	1.000	1.000	1.000	1.000	1.000	0.996	1.000	0.992	1.000	1.000
Plant Pot	0.996	0.996	1.000	1.000	0.998	0.998	0.998	1.000	1.000	0.996	0.996	0.996	0.996	1.000	0.992	0.996
Safety Sign	1.000	0.996	1.000	1.000	1.000	0.996	0.998	0.993	1.000	1.000	1.000	0.996	0.996	1.000	0.992	0.988
Scaffolding	1.000	1.000	1.000	1.000	1.000	1.000	1.000	1.000	1.000	1.000	1.000	1.000	1.000	1.000	1.000	1.000
Shrub	1.000	0.996	1.000	1.000	1.000	1.000	1.000	1.000	1.000	1.000	1.000	0.988	1.000	0.988	1.000	1.000
Table	1.000	1.000	1.000	1.000	1.000	1.000	1.000	1.000	1.000	1.000	1.000	1.000	1.000	1.000	0.992	0.996
Traffic Cone	1.000	1.000	1.000	1.000	1.000	1.000	1.000	1.000	1.000	1.000	1.000	1.000	1.000	1.000	1.000	1.000
Tree	1.000	1.000	1.000	1.000	1.000	1.000	1.000	1.000	1.000	1.000	1.000	1.000	1.000	1.000	0.996	1.000

Table B2: Test accuracy per obstacle type for the last 8 DL models (F: Frozen layers, NF: Not-frozen layers).

Obstacle Type	Mobilenet V2		Mobilenet V3 Large		Mobilenet V3 Small		Resnet101		Resnet152		Resnet18		Resnet34		Resnet50	
	F	NF	F	NF	F	NF	F	NF	F	NF	F	NF	F	NF	F	NF
2-Wheel Vehicle	1.000	1.000	1.000	1.000	1.000	1.000	1.000	1.000	1.000	1.000	0.995	1.000	0.995	1.000	1.000	1.000
4-Wheel Vehicle	1.000	0.995	1.000	1.000	0.995	0.995	1.000	0.990	1.000	0.995	0.990	0.995	1.000	1.000	1.000	0.985
Advert Sign	1.000	1.000	1.000	1.000	1.000	0.995	1.000	0.995	1.000	0.995	0.995	0.995	1.000	0.995	1.000	1.000
Bench	1.000	0.990	1.000	1.000	1.000	1.000	1.000	1.000	0.995	1.000	1.000	1.000	1.000	1.000	1.000	0.995
Bin	1.000	1.000	1.000	1.000	0.995	1.000	1.000	1.000	1.000	1.000	1.000	1.000	1.000	1.000	1.000	1.000
Boulder	1.000	0.995	1.000	1.000	1.000	1.000	1.000	1.000	1.000	1.000	0.995	1.000	1.000	0.995	1.000	1.000
Bus Stop	1.000	0.995	0.995	1.000	1.000	0.995	1.000	1.000	0.995	1.000	1.000	0.995	1.000	1.000	0.995	1.000
Chair	1.000	1.000	1.000	1.000	1.000	0.995	0.995	1.000	0.995	0.990	1.000	1.000	0.995	1.000	1.000	0.995
Crack	1.000	0.995	1.000	0.995	1.000	1.000	1.000	0.995	0.995	1.000	0.995	1.000	1.000	1.000	1.000	1.000
Crowded Pavement	1.000	1.000	1.000	1.000	1.000	1.000	1.000	1.000	1.000	1.000	1.000	1.000	1.000	1.000	1.000	1.000
Fence	1.000	1.000	0.985	1.000	1.000	1.000	1.000	1.000	1.000	1.000	1.000	1.000	1.000	1.000	1.000	1.000
Flower	1.000	1.000	1.000	1.000	0.995	1.000	1.000	1.000	1.000	1.000	0.995	1.000	1.000	1.000	1.000	1.000
Hole/Pot-Hole	1.000	0.995	1.000	0.995	0.995	0.995	1.000	1.000	0.995	1.000	1.000	1.000	1.000	1.000	1.000	1.000
Information Tourist Sign	0.995	1.000	1.000	1.000	1.000	1.000	1.000	1.000	1.000	0.995	1.000	1.000	1.000	1.000	1.000	1.000
Light Fixture	0.995	0.995	1.000	1.000	0.995	1.000	0.990	1.000	1.000	1.000	0.995	0.995	0.995	0.990	1.000	1.000
Litter	0.995	0.995	0.995	0.995	0.995	0.995	0.995	0.995	1.000	0.995	0.995	0.995	0.995	0.995	0.995	0.995
Mail Box	1.000	1.000	1.000	1.000	1.000	0.995	1.000	1.000	1.000	0.995	0.995	1.000	1.000	1.000	0.995	1.000
Narrow Pavement	1.000	1.000	1.000	1.000	1.000	1.000	1.000	1.000	1.000	0.995	1.000	0.995	1.000	1.000	1.000	1.000
No Pavement	1.000	1.000	0.985	1.000	1.000	1.000	1.000	1.000	1.000	1.000	0.990	1.000	0.995	1.000	0.995	1.000
Parking Meter	1.000	0.995	0.985	1.000	1.000	0.995	1.000	0.995	1.000	0.995	1.000	1.000	1.000	0.990	1.000	1.000
Parking Prev. Barrier	1.000	1.000	1.000	1.000	0.995	1.000	0.995	1.000	1.000	1.000	1.000	1.000	1.000	0.995	1.000	1.000
Paver Broken	0.995	1.000	0.995	1.000	0.990	1.000	1.000	1.000	1.000	1.000	0.995	1.000	0.990	1.000	1.000	1.000
Plant Pot	0.995	1.000	1.000	1.000	1.000	1.000	0.990	1.000	1.000	1.000	0.995	0.990	0.985	1.000	0.995	0.995
Safety Sign	0.985	0.995	1.000	0.995	0.990	0.990	0.995	0.980	0.995	0.990	0.985	0.990	0.985	0.990	0.995	0.985
Scaffolding	1.000	1.000	1.000	0.995	1.000	1.000	1.000	1.000	1.000	0.995	1.000	0.995	1.000	1.000	1.000	1.000
Shrub	0.995	0.995	0.995	1.000	1.000	1.000	0.990	1.000	0.995	1.000	0.995	1.000	0.995	1.000	1.000	1.000
Table	1.000	1.000	1.000	1.000	1.000	1.000	0.995	1.000	1.000	1.000	1.000	1.000	1.000	1.000	1.000	1.000
Traffic Cone	1.000	1.000	1.000	1.000	1.000	1.000	1.000	1.000	1.000	1.000	1.000	1.000	1.000	1.000	1.000	1.000
Tree	1.000	0.995	1.000	1.000	1.000	1.000	0.995	1.000	1.000	1.000	0.995	1.000	0.995	1.000	1.000	1.000

References

- [1] Piercy, K.L., Troiano, R.P., Ballard, R.M., Carlson, S.A., Fulton, J.E., Galuska, D.A., George, S.M., Olson, R.D.: The Physical Activity Guidelines for Americans. *JAMA: The Journal of the American Medical Association* **320**(19), 2020–2028 (2018) <https://doi.org/10.1001/jama.2018.14854>
- [2] Haghghi, M., Nadrian, H., Sadeghi-Bazargani, H., Hdr, D.B., Bakhtari Aghdam, F.: Challenges Related to Pedestrian Safety: A Qualitative Study Identifying Iranian Residents' Perspectives. *International Journal of Injury Control and Safety Promotion* **27**(3), 327–335 (2020) <https://doi.org/10.1080/17457300.2020.1774621>
- [3] Angin, M., Ali, S.I.A.: Analysis of Factors Affecting Road Traffic Accidents in North Cyprus. *Engineering, Technology & Applied Science Research* **11**(6), 7938–7943 (2021) <https://doi.org/10.48084/etasr.4547>
- [4] Ding, Z., Shen, Z., Guo, N., Zhu, K., Long, J.: Evacuation through Area with Obstacle That Can Be Stepped over: Experimental Study. *Journal of Statistical Mechanics: Theory and Experiment* **2020**(2), 023404 (2020) <https://doi.org/10.1088/1742-5468/ab6a01>

[5] Thoma, M., Partaourides, H., Sreedharan, I., Theodosiou, Z., Michael, L., Lanitis, A.: Performance Assessment of Fine-Tuned Barrier Recognition Models in Varying Conditions. In: Tsapatsoulis, N., Lanitis, A., Pattichis, M., Pattichis, C., Kyrkou, C., Kyriacou, E., Theodosiou, Z., Panayides, A. (eds.) Computer Analysis of Images and Patterns. Lecture Notes in Computer Science, pp. 172–181. Springer, Cham (2023). https://doi.org/10.1007/978-3-031-44240-7_17

[6] Theodosiou, Z., Thoma, M., Partaourides, H., Lanitis, A.: A Systematic Approach for Developing a Robust Artwork Recognition Framework Using Smartphone Cameras. *Algorithms* **15**(9), 305 (2022) <https://doi.org/10.3390/a15090305>

[7] Mann, S., Kitani, K.M., Lee, Y.J., Ryoo, M.S., Fathi, A.: An Introduction to the 3rd Workshop on Egocentric (First-Person) Vision. In: 2014 IEEE Conference on Computer Vision and Pattern Recognition Workshops, pp. 827–832 (2014). <https://doi.org/10.1109/CVPRW.2014.133>

[8] Wang, Z., Tan, S., Zhang, L., Yang, J.: ObstacleWatch: Acoustic-Based Obstacle Collision Detection for Pedestrian Using Smartphone. *Proceedings of the ACM on Interactive, Mobile, Wearable and Ubiquitous Technologies* **2**(4), 1–22 (2018) <https://doi.org/10.1145/3287072>

[9] Jain, S., Borgiattino, C., Ren, Y., Gruteser, M., Chen, Y., Chiasseroni, C.F.: LookUp: Enabling Pedestrian Safety Services via Shoe Sensing. In: Proceedings of the 13th Annual International Conference on Mobile Systems, Applications, and Services. MobiSys '15, pp. 257–271. Association for Computing Machinery, New York, NY, USA (2015). <https://doi.org/10.1145/2742647.2742669>

[10] Liu, X., Cao, J., Wen, J., Tang, S.: InfraSee: An Unobtrusive Alertness System for Pedestrian Mobile Phone Users. *IEEE Transactions on Mobile Computing* **16**(2), 394–407 (2017) <https://doi.org/10.1109/TMC.2016.2550447>

[11] Wang, T., Cardone, G., Corradi, A., Torresani, L., Campbell, A.T.: WalkSafe: A Pedestrian Safety App for Mobile Phone Users Who Walk and Talk While Crossing Roads. In: Proceedings of the Twelfth Workshop on Mobile Computing Systems & Applications. HotMobile '12, pp. 1–6. Association for Computing Machinery, New York, NY, USA (2012). <https://doi.org/10.1145/2162081.2162089>

[12] Tang, M., Nguyen, C.-T., Wang, X., Lu, S.: An Efficient Walking Safety Service for Distracted Mobile Users. In: 2016 IEEE 13th International Conference on Mobile Ad Hoc and Sensor Systems (MASS), pp. 84–91 (2016). <https://doi.org/10.1109/MASS.2016.021>

[13] Jain, S., Gruteser, M.: Recognizing Textures with Mobile Cameras for Pedestrian Safety Applications. *IEEE Transactions on Mobile Computing* **18**(8), 1911–1923 (2019) <https://doi.org/10.1109/TMC.2018.2868659>

[14] Wei, Z., Lo, S.-W., Liang, Y., Li, T., Shen, J., Deng, R.H.: Automatic Accident

Detection and Alarm System. In: Proceedings of the 23rd ACM International Conference on Multimedia. MM '15, pp. 781–784. Association for Computing Machinery, New York, NY, USA (2015). <https://doi.org/10.1145/2733373.2807402>

[15] Foerster, K.-T., Gross, A., Hail, N., Uitto, J., Wattenhofer, R.: SpareEye: Enhancing the Safety of Inattentionally Blind Smartphone Users. In: Proceedings of the 13th International Conference on Mobile and Ubiquitous Multimedia. MUM '14, pp. 68–72. Association for Computing Machinery, New York, NY, USA (2014). <https://doi.org/10.1145/2677972.2677973>

[16] Hasan, R., Hasan, R.: Pedestrian Safety Using the Internet of Things and Sensors: Issues, Challenges, and Open Problems. Future Generation Computer Systems **134**, 187–203 (2022) <https://doi.org/10.1016/j.future.2022.03.036>

[17] Theodosiou, Z., Partaourides, H., Atun, T., Panayi, S., Lanitis, A.: A First-Person Database for Detecting Barriers for Pedestrians. In: VISIGRAPP 2020 - Proceedings of the 15th International Joint Conference on Computer Vision, Imaging and Computer Graphics Theory and Applications, vol. 5, pp. 660–666 (2020). <https://doi.org/10.5220/0009107506600666>

[18] Simonyan, K., Zisserman, A.: Very Deep Convolutional Networks for Large-Scale Image Recognition. arXiv (2015). <https://doi.org/10.48550/arXiv.1409.1556>

[19] Thoma, M., Theodosiou, Z., Partaourides, H., Tylliros, C., Antoniades, D., Lanitis, A.: A Smartphone Application Designed to Detect Obstacles for Pedestrians' Safety. In: Paiva, S., Lopes, S.I., Zitouni, R., Gupta, N., Lopes, S.F., Yonezawa, T. (eds.) Science and Technologies for Smart Cities. Lecture Notes of the Institute for Computer Sciences, Social Informatics and Telecommunications Engineering, pp. 358–371. Springer, Cham (2021). https://doi.org/10.1007/978-3-030-76063-2_25

[20] Theodosiou, Z., Partaourides, H., Panayi, S., Kitsis, A., Lanitis, A.: Detection and Recognition of Barriers in Egocentric Images for Safe Urban Sidewalks. In: Bouatouch, K., de Sousa, A.A., Chessa, M., Paljic, A., Kerren, A., Hurter, C., Farinella, G.M., Radeva, P., Braz, J. (eds.) Computer Vision, Imaging and Computer Graphics Theory and Applications. Communications in Computer and Information Science, pp. 530–543. Springer, Cham (2022). https://doi.org/10.1007/978-3-030-94893-1_25

[21] Ren, S., He, K., Girshick, R., Sun, J.: Faster R-CNN: Towards Real-Time Object Detection with Region Proposal Networks. IEEE Transactions on Pattern Analysis and Machine Intelligence **39**(6), 1137–1149 (2017) <https://doi.org/10.1109/TPAMI.2016.2577031>

[22] Szegedy, C., Vanhoucke, V., Ioffe, S., Shlens, J., Wojna, Z.: Rethinking the Inception Architecture for Computer Vision. In: 2016 IEEE Conference on Computer Vision and Pattern Recognition (CVPR), pp. 2818–2826 (2016). <https://doi.org/10.1109/CVPR.2016.308>

- [23] He, K., Zhang, X., Ren, S., Sun, J.: Deep Residual Learning for Image Recognition. arXiv (2015). <https://doi.org/10.48550/arXiv.1512.03385>
- [24] Liu, W., Anguelov, D., Erhan, D., Szegedy, C., Reed, S., Fu, C.-Y., Berg, A.C.: SSD: Single Shot MultiBox Detector. In: Leibe, B., Matas, J., Sebe, N., Welling, M. (eds.) Computer Vision – ECCV 2016, pp. 21–37. Springer, Cham (2016). https://doi.org/10.1007/978-3-319-46448-0_2
- [25] Sandler, M., Howard, A., Zhu, M., Zhmoginov, A., Chen, L.-C.: MobileNetV2: Inverted Residuals and Linear Bottlenecks. In: Proceedings of the IEEE Conference on Computer Vision and Pattern Recognition, pp. 4510–4520 (2018). <https://doi.org/10.1109/CVPR.2018.00474>
- [26] Damen, D., Doughty, H., Farinella, G.M., Furnari, A., Kazakos, E., Ma, J., Moltisanti, D., Munro, J., Perrett, T., Price, W., Wray, M.: Rescaling Egocentric Vision: Collection, Pipeline and Challenges for EPIC-KITCHENS-100. International Journal of Computer Vision **130**(1), 33–55 (2022) <https://doi.org/10.1007/s11263-021-01531-2>
- [27] Grauman, K., Westbury, A., Byrne, E., Chavis, Z., Furnari, A., Girdhar, R., Hamburger, J., Jiang, H., Liu, M., Liu, X., *et al.*: Ego4D: Around the World in 3,000 Hours of Egocentric Video. In: Proceedings of the IEEE/CVF Conference on Computer Vision and Pattern Recognition, pp. 18973–18990 (2022). <https://doi.org/10.1109/CVPR52688.2022.01842>
- [28] Sigurdsson, G.A., Gupta, A., Schmid, C., Farhadi, A., Alahari, K.: Actor and Observer: Joint Modeling of First and Third-Person Videos. In: Proceedings of the IEEE Conference on Computer Vision and Pattern Recognition, pp. 7396–7404 (2018). https://openaccess.thecvf.com/content_cvpr_2018/html/Sigurdsson_Actor_and_Observer_CVPR_2018_paper.html
- [29] Li, Y., Liu, M., Rehg, J.M.: In the Eye of Beholder: Joint Learning of Gaze and Actions in First Person Video. In: Proceedings of the European Conference on Computer Vision (ECCV), pp. 619–635 (2018). https://openaccess.thecvf.com/content_ECCV_2018/html/Yin_Li_In_the_Eye_ECCV_2018_paper.html
- [30] Lee, Y.J., Ghosh, J., Grauman, K.: Discovering Important People and Objects for Egocentric Video Summarization. In: 2012 IEEE Conference on Computer Vision and Pattern Recognition, pp. 1346–1353 (2012). <https://doi.org/10.1109/CVPR.2012.6247820>
- [31] Zhu, C., Xiao, F., Alvarado, A., Babaei, Y., Hu, J., El-Mohri, H., Culatana, S., Sumbaly, R., Yan, Z.: EgoObjects: A Large-Scale Egocentric Dataset for Fine-Grained Object Understanding. In: Proceedings of the IEEE/CVF International Conference on Computer Vision, pp. 20110–20120 (2023). https://openaccess.thecvf.com/content/ICCV2023/html/Zhu_EgoObjects_A_Large-Scale_Egocentric_Dataset_for_Fine-Grained_Object_Understanding_ICCV_2023_paper.html

- [32] Zhang, Y., Cao, C., Cheng, J., Lu, H.: EgoGesture: A New Dataset and Benchmark for Egocentric Hand Gesture Recognition. *IEEE Transactions on Multimedia* **20**(5), 1038–1050 (2018) <https://doi.org/10.1109/TMM.2018.2808769>
- [33] Palazzi, A., Abati, D., Calderara, S., Solera, F., Cucchiara, R.: Predicting the Driver’s Focus of Attention: The DR(Eye)VE Project. *IEEE Transactions on Pattern Analysis and Machine Intelligence* **41**(7), 1720–1733 (2019) <https://doi.org/10.1109/TPAMI.2018.2845370>
- [34] Ragusa, F., Furnari, A., Battiatto, S., Signorello, G., Farinella, G.M.: EGO-CH: Dataset and Fundamental Tasks for Visitors Behavioral Understanding Using Egocentric Vision. *CoRR* **abs/2002.00899** (2020) [arxiv:2002.00899](https://arxiv.org/abs/2002.00899)
- [35] Dunnhofer, M., Furnari, A., Farinella, G.M., Micheloni, C.: Visual Object Tracking in First Person Vision. *International Journal of Computer Vision* **131**(1), 259–283 (2023) <https://doi.org/10.1007/s11263-022-01694-6>
- [36] Howard, A., Sandler, M., Chu, G., Chen, L.-C., Chen, B., Tan, M., Wang, W., Zhu, Y., Pang, R., Vasudevan, V., Le, Q.V., Adam, H.: Searching for MobileNetV3. *arXiv* (2019). <https://doi.org/10.48550/arXiv.1905.02244>
- [37] Dosovitskiy, A., Beyer, L., Kolesnikov, A., Weissenborn, D., Zhai, X., Unterthiner, T., Dehghani, M., Minderer, M., Heigold, G., Gelly, S., Uszkoreit, J., Houlsby, N.: An Image Is Worth 16x16 Words: Transformers for Image Recognition at Scale. In: *International Conference on Learning Representations (ICLR 2021)*, Virtual Event, Austria (2021). <https://openreview.net/forum?id=YicbFdNTTy>
- [38] Vaswani, A., Shazeer, N., Parmar, N., Uszkoreit, J., Jones, L., Gomez, A.N., Kaiser, Ł., Polosukhin, I.: Attention Is All You Need. In: *Advances in Neural Information Processing Systems*, vol. 30. Curran Associates, Inc., Long Beach, CA, USA (2017). https://proceedings.neurips.cc/paper_files/paper/2017/hash/3f5ee243547dee91fbd053c1c4a845aa-Abstract.html
- [39] Council of the European Union, European Parliament: Regulation (EU) 2016/679 of the European Parliament and of the Council of 27 April 2016 on the Protection of Natural Persons with Regard to the Processing of Personal Data and on the Free Movement of Such Data, and Repealing Directive 95/46/EC (General Data Protection Regulation) (Text with EEA Relevance), OJ L 119, 4.5.2016, p. 1–88 (2016). <https://eur-lex.europa.eu/eli/reg/2016/679/2016-05-04>
- [40] Tan, M., Le, Q.V.: EfficientNet: Rethinking Model Scaling for Convolutional Neural Networks. *arXiv* (2020). <https://doi.org/10.48550/arXiv.1905.11946>
- [41] Szegedy, C., Liu, W., Jia, Y., Sermanet, P., Reed, S., Anguelov, D., Erhan, D., Vanhoucke, V., Rabinovich, A.: Going Deeper with Convolutions. *arXiv* (2014). <https://doi.org/10.48550/arXiv.1409.4842>

- [42] Huang, G., Liu, Z., van der Maaten, L., Weinberger, K.Q.: Densely Connected Convolutional Networks. In: Proceedings of the IEEE Conference on Computer Vision and Pattern Recognition, pp. 4700–4708 (2017). https://openaccess.thecvf.com/content_cvpr_2017/html/Huang_Densely_Connected_Convolutional_CVPR_2017_paper.html
- [43] Tan, M., Le, Q.: EfficientNetV2: Smaller Models and Faster Training. In: Proceedings of the 38th International Conference on Machine Learning, pp. 10096–10106. PMLR, Virtual Event (2021). <https://proceedings.mlr.press/v139/tan21a.html>
- [44] Liu, Z., Mao, H., Wu, C.-Y., Feichtenhofer, C., Darrell, T., Xie, S.: A ConvNet for the 2020s. In: Proceedings of the IEEE/CVF Conference on Computer Vision and Pattern Recognition, pp. 11976–11986 (2022). https://openaccess.thecvf.com/content/CVPR2022/html/Liu_A_ConvNet_for_the_2020s_CVPR_2022_paper.html
- [45] Deng, J., Dong, W., Socher, R., Li, L.-J., Li, K., Fei-Fei, L.: ImageNet: A Large-Scale Hierarchical Image Database. In: 2009 IEEE Conference on Computer Vision and Pattern Recognition, pp. 248–255 (2009). <https://doi.org/10.1109/CVPR.2009.5206848>
- [46] Russakovsky, O., Deng, J., Su, H., Krause, J., Satheesh, S., Ma, S., Huang, Z., Karpathy, A., Khosla, A., Bernstein, M., Berg, A.C., Fei-Fei, L.: ImageNet Large Scale Visual Recognition Challenge. International Journal of Computer Vision **115**(3), 211–252 (2015) <https://doi.org/10.1007/s11263-015-0816-y>
- [47] Kingma, D.P., Ba, J.: Adam: A Method for Stochastic Optimization. arXiv (2017). <https://doi.org/10.48550/arXiv.1412.6980>
- [48] Thoma, M., Theodosiou, Z., Partaourides, H., Vassiliades, V., Loizos, M., Lanitis, A.: PEDESTRIAN: An Egocentric Vision Dataset for Obstacle Detection. Zenodo (2025). <https://doi.org/10.5281/zenodo.10907945>